SOILS AND FOUNDATIONS Vol. 45, No. 3, 97–105, June 2005
Japanese Geotechnical Society

CONSOLIDATION BEHAVIOR OF NATURAL SOILS AROUND p_c VALUE – INTER-CONNECTED OEDOMETER TEST –

HIROYUKI TANAKA[i)]

ABSTRACT

It has been known from the conventional oedometer test that considerable settlement is observed after the end of primary consolidation, i.e., under the constant effective stresses. One of the most controversial issues in the geotechnical engineering is whether such secondary compression is taking place during and/or after the dissipation of the excess pore water pressure. Using the Pleistocene clays recovered from the Osaka basin, Long Term Consolidation (LTC) and Inter-Connected Oedometer (ICO) tests were carried out. This paper presents the consolidation behavior measured by the ICO and the companion paper will deal with the findings obtained by the LTC. The main advantage of the ICO test is its ability to investigate the influences of drainage path length under conditions of relatively small friction between the specimen and the oedometer ring. It was found that dissipation of the excess pore water pressure follows the H^2 rule, regardless of the relative stress range, i.e., at over- or normally consolidated state, where the H is the thickness of the specimen. However, the generated strain at overconsolidated state does not follow the H^2 rule. These test results were tried to be explained by the strain rate theory.

Key words: consolidation, drainage length path, inter-connected oedometer test, Pleistocene clay, secondary compression, strain rate (**IGC**: D5)

INTRODUCTION

As described in the companion paper (Tanaka, 2005), when the consolidation pressure is around the yield pressure (p_c)[1] for normally aged consolidated clay such as Osaka Pleistocene clays, the significant settlement is generated after the dissipation of the excess water pressure: i.e., the secondary compression[2] is prominent. One of the most controversial issues in Geotechnical engineering has been whether such secondary compression takes place during and/or after the primary consolidation, since Ladd et al. (1977) reviewed in their state of the art at the Tokyo ICSMFE, in the name of the Hypotheses A or B. As shown in Fig. 1, in Hypothesis A, the relation between the strain and effective stress is uniquely defined, and the end of primary consolidation (EOP) is defined irrespective of the objective layer thickness. Thus, the secondary compression is generated after the EOP. Following Hypothesis A, when applying test result from the laboratory to the field, in which the objective layer is much more thicker than that at laboratory, speed of consolidation in the primary consolidation can be calculated by the hydrodynamic equation, that is, the degree of consolidation (U) follows the H^2 theory, and the subsequent secondary compression is calculated by $C_\alpha \log(t/t_p)$, where C_α is the coefficient of the secondary compression and t_p is the time for the EOP. On the other hand, in Hypothesis B, the relation between strain and effective stress cannot be uniquely defined and the secondary compression, in other word, the strain due to creep, is generated during and after the dissipation of the excess pore water pressure. Therefore, in this hypothesis, the EOP cannot be uniquely defined and the strain at the EOP increases with

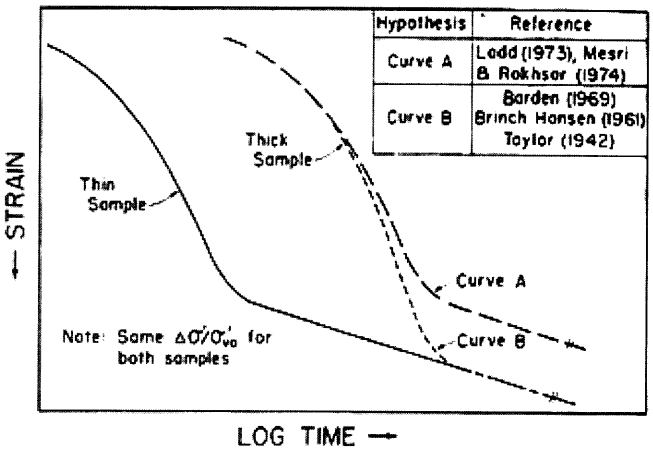

Fig. 1. Hypothesis A and B (after Ladd et al., 1977)

[1]The p_c value in this paper is obtained by the Constant Rate of Strain oedometer test with a strain rate of $3.3 \times 10^{-6}\,s^{-1}$, as described later.
[2]In this paper, the settlement or volume change under constant effective stresses is called "secondary compression".

i) Hokkaido University, Japan (tanaka@eng.hokudai.ac.jp) (formerly Port and Airport Research Institute, Japan).
The manuscript for this paper was received for review on February 20, 2004; approved on January 18, 2005.
Written discussions on this paper should be submitted before January 1, 2006 to the Japanese Geotechnical Society, 4-38-2, Sengoku, Bunkyo-ku, Tokyo 112-0011, Japan. Upon request the closing date may be extended one month.

an increase in thickness of the compressible layer. The difference in settlement estimated based on Hypothesis A and B becomes significant when the component of the secondary compression in the total settlement is large, for example, in case the consolidation pressure is close to the p_c value.

The validity of these hypotheses has been examined by many researchers, using different thickness of the soil specimen for consolidation test (for example, Aboshi, 1973; Mesri et al., 1994). The main problem in large thickness of the specimen is the friction between the oedometer ring and the specimen. For the sake of minimization of the friction, the Inter-Connected Oedometer (ICO) test has been carried out by, for example, Berre and Iversen (1972), Aboshi et al. (1981), and Imai and Tan (1992).

In the present study, the soil specimen is divided into several elements with thickness of 1 or 2 cm so that the friction can be considerably reduced. In addition to the reduction of the friction, another important advantage of the ICO apparatus is its ability to measure strains and pore water pressures in the specimen having a different drainage length during the consolidation. Unlike the triaxial test when the specimen is sheared, the generated strains or effective stresses in the specimen in the oedometer ring are not uniform because the excess pore water pressure is first dissipated from the drainage side.

It has been revealed from previous studies using different thickness of specimens that the strain is not only defined by the effective stress, but also by the strain rate (for example, Imai and Tan, 1992). That is, the EOP cannot be uniquely defined, but is dependent on the thickness of the compressible layer. However, these studies mostly have been carried out for reconstituted samples and the applied load is in the range of normally consolidated state. Few studies have been carried out on the intact samples.

This paper will present the consolidation behavior of intact samples at the consolidation pressure around the p_c value, using the ICO apparatus. The companion paper (Tanaka, 2005) will present consolidation test results from the long term consolidation test.

CLAYS INVESTIGATED AND TESTING METHOD

In this study, Osaka Pleistocene clays, namely, Ma10 and Ma3, were used. Table 1 gives the main consolidation parameters as well as the index properties of clays used in this study. Indeed, in this study, other Ma layers, namely Ma12 and Ma7, were also used. As will be described later, however, several holes created by marine animals were found in these specimens and their existence gives significant influence on the test results. Therefore, in this paper, only test results from Ma10 and Ma3 are presented. More detailed description of the Pleistocene clay layers and their properties may be referred in many literatures, for example, Itoh et al. (2000); Tanaka et al. (2004) and the companion paper (Tanaka, 2005). These clays were retrieved by a hydraulic piston sampler for Ma10 and by a triple tubes core sampler for Ma3. These different sampling methods were employed to cater the stiffness differences of these clay layers.

Table 1. Properties of soils used in the test

Layer	Ma10	Ma3
Elevation (COD m)	125	276
Sample No.	T86	D149
p'_{vo} (kPa)	760	1950
p_c (kPa)	960	2540
OCR	1.26	1.30
C_{cmax}	1.02	2.74
C_{c1}	0.76	0.65
e_0	1.35	1.68
w_L (%)	103	108
w_P (%)	39	39
w_n (%)	50.9	61.9

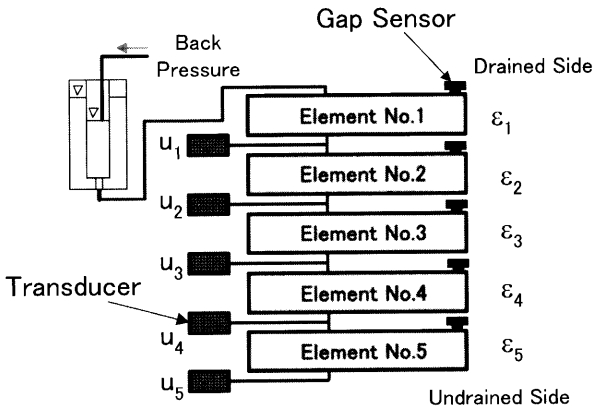

(a) System of the inter-connected oedometer test. The figure shows the case consisting of 5 chambers

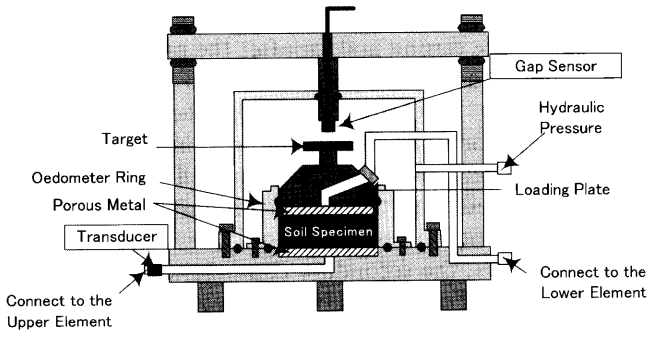

(b) Detail figure of the chamber of the inter-connected oedometer

Fig. 2. Schematic views of inter-connected oedometer apparatus

The Inter-Connected Oedometer (ICO) apparatus used in this study is schematically illustrated in Fig. 2. The diameter of the oedometer ring is 60 mm, which is the same as the conventional oedometer test. The initial

Table 2. Series of inter-connected oedometer tests

(a) Stress level is at normally consolidated state

Test number	H2	H5	H10
Layer	Ma10		
Load range	$2p_c - 3p_c$		
Total thickness (cm)	2.0	5.0	10.0
Num. of element	2	5	5
Thickness of element (cm)	1.0	1.0	2.0
Duration of precon. ($\times 10^4$ s)	1.4	9.0	34.6

(b) Stress level is at overconsolidated state

Test number	H2	H5	H10	H20
Layer	Ma3			
Load range	$p'_{vo} - p_c$			
Total thickness (cm)	2.0	5.0	10.0	20.0
Num. of element	2	5	5	10
Thickness of element (cm)	1.0	1.0	2.0	2.0
Duration of precon. ($\times 10^4$ s)	1.4	8.7	37.5	325

height of the specimen is 10 mm or 20 mm, depending on the purpose of the test (*see* Table 2). Each oedometer ring was connected by a copper tube to minimize the volume change due to the change in the excess pore water pressure. The change of the water pressure was measured by the diaphragm type of the water pressure measuring device, which was equipped in the copper tube between oedometer rings. The consolidation pressure was applied by water pressure. A backpressure of 200 kPa was applied to ensure high degree of saturation of the specimen. The settlement of each oedometer ring was measured by a gap sensor. The maximum number of inter-connected oedometer element was 10. The total thickness and the number of elements for the test are given in Table 2.

In this paper, the soil element is numbered in the order from the drained side. For example, in the test number H10 (*see* Table 2), where the total thickness of the specimens (H) is 10 cm and consists of 5 soil elements (the thickness of each soil element being 2 cm), the soil element No. 1 is located at the drained side. On the other hand, the element No. 5 has the longest drainage length. H1 may correspond to the conventional oedometer test with 2 cm thickness, because its both sides are drained. The strain and the strain rate measured in the element No. 1, for example, are named as ε_1 and $\dot{\varepsilon}_1$, respectively. The pore water pressure is also named as u_1, which was measured between the elements No. 1 and No. 2. Similarly, the u_5 was measured at the undrained side of the No. 5 element.

Using Ma3 sample, the consolidation behavior around the p_c value is studied. The specimen was first consolidated under p'_{vo} (whose duration time for the pre-consolidation is given in Table 2), then the pressure was increased to the corresponding p_c value, as measured by constant rate of strain (CRS) oedometer test, at a strain rate of 3.3×10^{-6} s^{-1}. The consolidation behavior under the normally consolidated state has also been studied using the Ma10 sample. Figure 3 shows the $e - \log p$ relation measured by the CRS test and the range of applied load for Ma3 and Ma10 samples by arrows. It should be kept in mind that change in the void ratio for Ma3 would be definitely smaller than that for Ma10, if we estimate the volume change from the CRS test result.

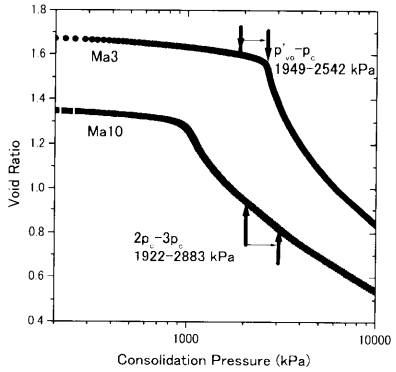

Fig. 3. $e - \log p$ relations determined by CRS for soils used in this study and their stress ranges applied in the ICO test

In order to obtain consolidation properties as a reference, CRS test was carried out under a strain rate of 3.3×10^{-6} s^{-1} (0.02%/min), as mentioned above. The size of the specimen used was 60 mm in diameter and 20 mm in initial height. A backpressure of 200 kPa was applied. Pore water pressure was measured at the bottom of the specimen, while the drainage was allowed at the upper part of the specimen. The effective consolidation stress (p') was calculated assuming that the pore water pressure is distributed in the parabolic manner: $p' = p - 2/3\,u$, where p is the measured total applied pressure and u is the pore water pressure measured at the bottom of the specimen.

TEST RESULTS

Effect of Heterogeneity of Specimens

One of the serious obstacles in using intact samples may be heterogeneity of samples used in the test. Especially, in this study, a long core sample is required to carry out a series of tests. Figure 4 shows the variation in initial water content (w_i) of each element. It may be anticipated from the variation of w_i in these elements that the consolidation properties could also vary for each element. This figure also shows the generated strains before the test is started (for Ma3, at p'_{vo}; for Ma10, at $2p_c$) as well as after the objective test is finished. It was anticipated that the strain in elements located near the drained side would be much larger than that near the undrained side, because the duration of the secondary consolidation in the vicinity of the drainage is expected to be much longer. However, a systematic variation in the

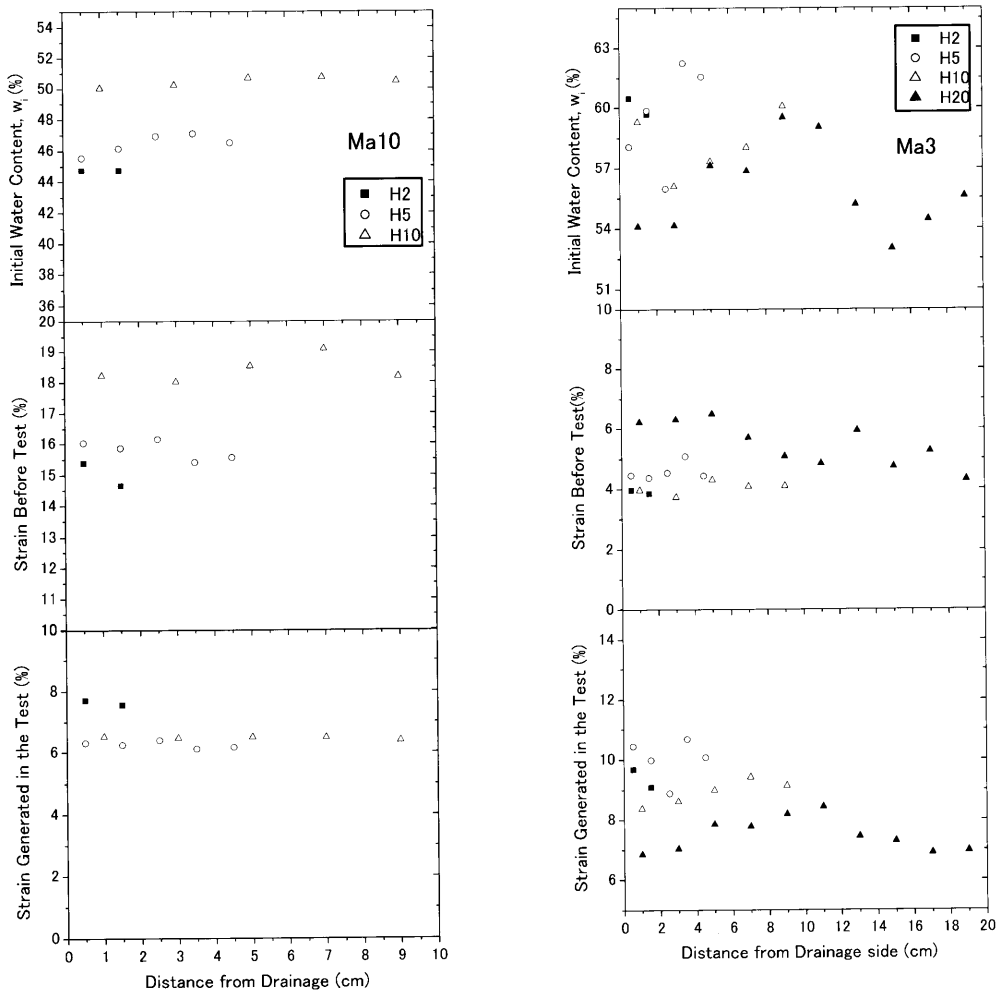

(a) Ma10 (b) Ma3

Fig. 4. Initial water content and generated strain for each soil elements

strains during the preloading (before the testing) as well as at the objective stress level can not be recognized. This fact indicates that the influence of heterogeneity in the soil element is much more significant than that of location of the elements. It is also confirmed that duration of the test is long enough to ignore the difference in the drainage lengths of each element.

Validity of Darcy's Law (Influence of Holes Created by Marine Animals' Activity)

This paper describes only two test series namely Ma10 and Ma3, where their stress levels range from $2p_c$ to $3p_c$ for Ma10, and from p'_{vo} to p_c for Ma3. In addition to these test series, other tests using other Ma layers as well as different stress levels were also carried out in this study. In some of these tests, strange behavior was observed in the process of the excess pore water pressure dissipation. A typical example is shown in Fig. 5, where the total thickness of the specimen was 20 cm and the stress level was increased from p'_{vo} to 1.1 times as large as the p_c value. The soil sample was retrieved from the Ma7 layer. Although the 10 elements were used in this test, the figure

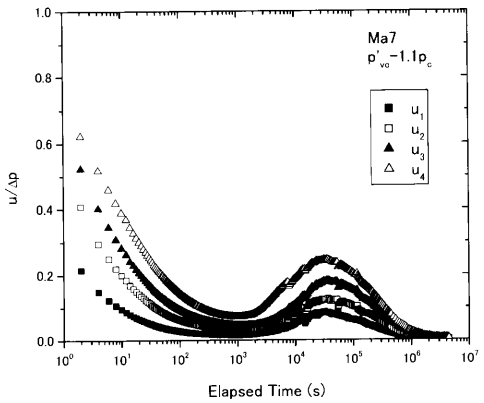

Fig. 5. An example of the relationships between elapsed time and excess pore water pressure in each soil element

shows only the test result for No.1 to No.4 elements.

After the excess pore water pressures rapidly dissipated until 2000 seconds, they rose again and reached the peak after 30,000 seconds. As described in the companion paper as well as other papers (*see* for example, Tanaka

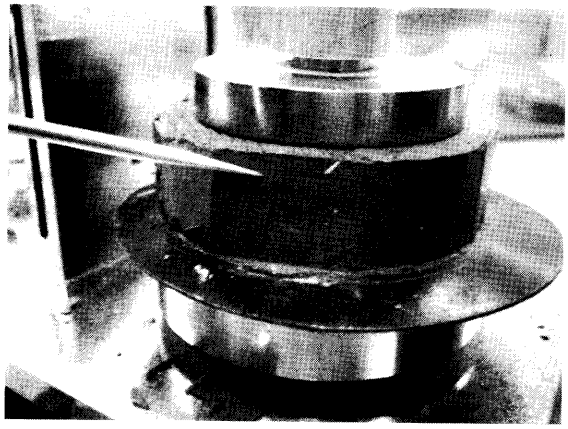

Photo 1. Typical example of existence of hole created by the marine life's activity

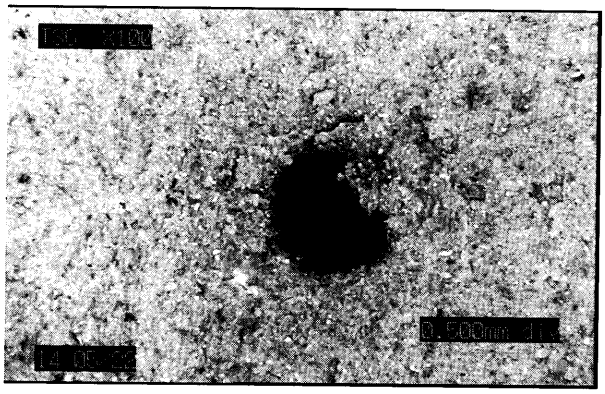

Photo 2. Magnification of the hole: The diameter of this hole is about 0.5 mm

and Locat, 1999; Tanaka et al., 2004), the Osaka Pleistocene clays have relatively large void ratio with respect to the p'_{vo}: i.e., their structure is well developed. Thus, it was initially anticipated that Fig. 5 would show a good evidence of the collapse of such highly developed structures, so that the excess pore water pressures would be generated even though the time has elapsed. When the specimens were carefully examined after the test, however, a lot of small holes were found in the specimens, and they were probably made by activities of marine lives such as worms, as shown in Photos 1 and 2. It was surprising to realize that these holes remained even under a high p'_{vo} of the Ma7 layer (about 1.5 MPa). It is inferred that the generated excess pore water was rapidly dissipated in the early stage because of the small holes. With the progress of the consolidation, however, when the effective stress reaches the p_c value, the hole collapsed and the resulting permeability is considerably reduced. Such reduction of drainage function of the holes may cause the rise of the excess pore water pressure.

In order to examine the influence of these life traces on the test result, the process of dissipation of the excess pore water pressure was studied from a viewpoint of the Darcy's law. According to the Darcy's law, the relation may be established among v, i and k, as shown in the following equation.

$$v = ki \tag{1}$$

where v is the apparent velocity of the fluid, k is the hydraulic conductivity and i is the hydraulic gradient. The value of v may be obtained by the summation of the volume change in the soil elements located up stream from the objective soil element for a certain time duration. The volume change in each soil element can be obtained by displacement from the gap sensor equipped in the chamber, as described earlier. The amount of v obtained in this manner is flown into the boundary of the up stream side of the objective soil element. The value of i is assumed to be constant in the soil element and may be calculated from the pore water pressures measured at both boundary sides of the objective element: i.e., $i = (u_{up} - u_{down} - \gamma_w h)/h$, where u_{up} and u_{down} are the pore water pressures at the up and the down stream sides of the element, respectively. This assumption is not correct, especially at the initial consolidation stage and when the element is not thin enough. However, after a certain time elapses, the hydraulic gradient may be approximately expressed by the above equation, except for the element close to the drainage boundary. This point will be further discussed later. The h and γ_w are the thickness of the soil element, and the unit weight of fluid, respectively.

Figure 6(a) shows the relation between i and v for Ma7, corresponding to the relation between the elapsed time and $u/\Delta p$ shown in Fig. 5. The relation for Ma3, which is presented and analyzed in this paper, is also shown in Fig. 6(b) for the purpose of comparison. As can be seen in the case of Ma7, where the holes are found and the rise of the pore water pressure is recognized during the consolidation, the value of v is very large with respect to i at the initial stage, because of large permeability caused by the holes. But as consolidation proceeds and the holes are gradually collapsed, the value of v decreases in spite of increase in i. When the holes are completely collapsed, the relation between v and i becomes linear and its gradient may correspond to k value ($= 1.4 \times 10^{-10}$ m/s in the figure) of the soil element. On the other hand, Ma3, in which such holes were not recognized in the specimens, shows completely opposite tendency compared to that of Ma7. That is, at the first stage, the order of v is relatively low in spite of high i. This may be because the value of i is assumed to be constant in the soil element. At early stages of the consolidation, as the distribution of u is not straight, but somewhat convex so that the i at the up stream side of the element is smaller than that calculated by $i = (u_{up} - u_{down} - \gamma_w h)/h$. As the consolidation proceeds, however, the value of i can be reasonably estimated from the assumption of constant i in the soil element. Then, it is observed that the v follows the Darcy's law ($k = 9.1 \times 10^{-11}$ m/s in the figure).

The value of k measured by the CRS test is compared in Fig. 7, with the values of k obtained from the ICO test, when the relation between i and v becomes constant. In this figure, the k value measured by the CRS apparatus

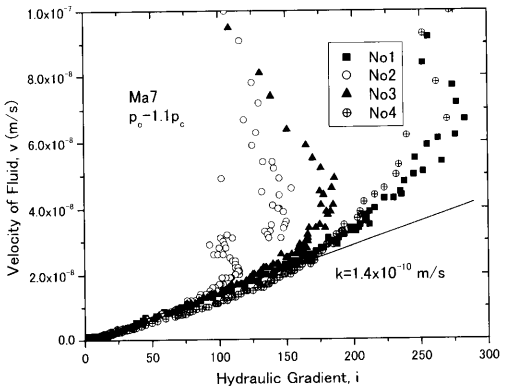

(a) Case with existence of holes created by marine animals

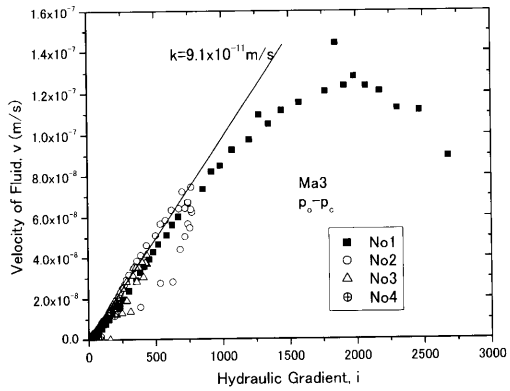

(b) Case without holes

Fig. 6. Validity of Darcy's law during consolidation in the interconnected oedometer

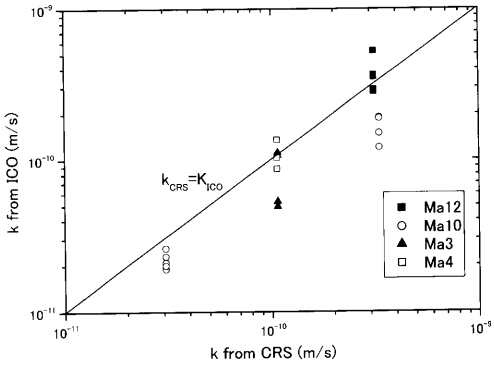

Fig. 7. Comparison of hydraulic coefficient measured by the interconnected oedometer and Constant Rate of Strain oedometer tests

is the value in the same stress range as that of the ICO test. A good correlation between these k values can be recognized in Fig. 7. It is thus confirmed that test results from Ma10 and Ma3 are not influenced by the existence of holes such as Ma7 in Fig. 6(a), and they are reliable enough for the analysis.

Influence of Thickness

Figure 8(a) shows the influence of the specimen

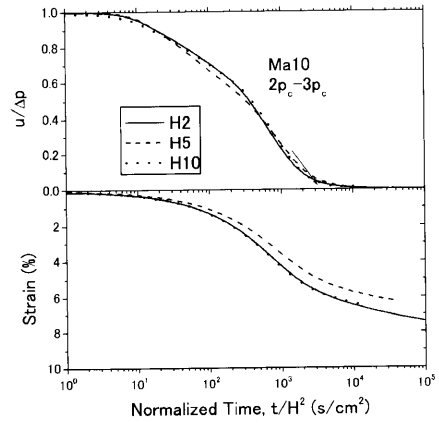

(a) Ma10: The stress range is at normally consolidated state

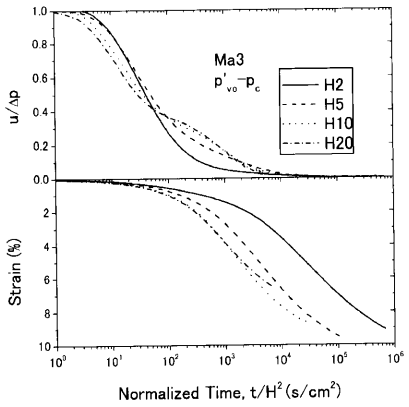

(b) Ma3: The stress range is at overconsolidated state

Fig. 8. Relationships between elapsed time and the excess pore water pressure (u), or total strain: The time is normalized by H^2, where H is thickness of the specimen: The u is measured at the bottom in undrained condition

thickness on the relation between strain and time, as well as on the relation between dissipation of the excess pore water and time, for normally consolidated (NC) states. In the figure, time is normalized by square of the total thickness of specimen, H^2, considering the hydrodynamic equation. The excess pore water pressure was measured at the undrained side and normalized by the applied consolidation pressure (Δp), i.e., $u/\Delta p$. Similarly, the relation for Ma3, whose stress range is between p'_{vo} and p_c, is presented in Fig. 8(b). The relations obtained from the NC state are much more familiar in the conventional soil mechanics, as described in typical textbooks. That is, both $u/\Delta p$ and strain can be normalized by H^2. In addition to such normalization of $u/\Delta p$ as well as strain, it can be seen that the strain is generated simultaneously with dissipation of the excess pore water pressure, i.e., an increase in the effective stress.

On the other hand, the behavior of Ma3, in which the consolidation pressure increases from p'_{vo} to p_c, is completely different from that of the NC state. It is apparent that the dissipation of $u/\Delta p$ is normalized by the H^2. However, if we take a look at the figure in more detail, it is found that as H increases, the rate of dissipa-

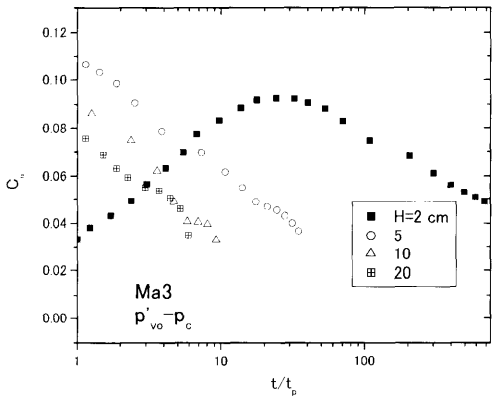

Fig. 9. Dependency of the coefficient of secondary compression on the thickness of the specimen

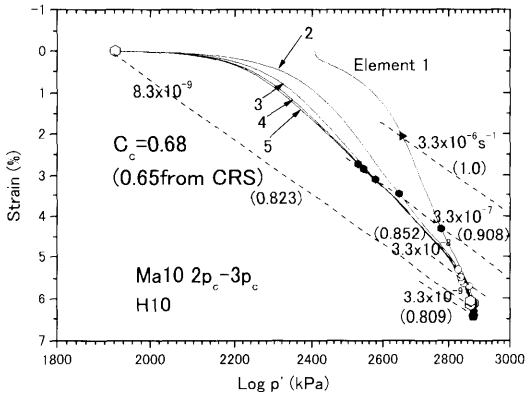

(a) Ma10: The stress range is at normally consolidated state

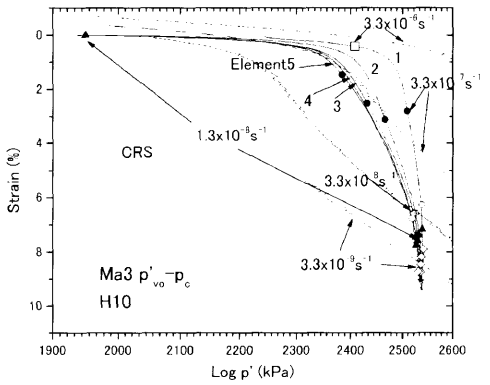

(b) Ma3: The stress range is at overconsolidated state

Fig. 10. Stress and strain relation in soil elements during the inter-connected oedometer test

tion of the excess pore water pressure is retarded at $u/\Delta p$ of 0.4. This retardation is not caused by the existence of holes in the specimen as described previously, because even in such a situation the Darcy's law can be applied as shown in Fig. 6(b).

The strain cannot be related to the normalized time by H^2. As H increases, the strain increases more rapidly. The most interesting point is that the strain at dissipation of the excess pore water pressure is very small, and most part of the strain is yielded after the dissipation of the excess pore water pressure. For example, in case of $H=2$ cm, when $u/\Delta p$ is 0.1, the normalized time is 300 s/cm^2. At this time, strain is only 0.8%. However, as time proceeds at t/H^2 of 100,000 s/cm^2, the strain reaches to as much as 7%. As reported in the companion paper, when consolidation pressure is close to the p_c value, most of the settlement takes place after the end of the primary consolidation. The present study confirms again this fact by measuring the excess pore water pressure. As H increases, it seems that the portion of the settlement associated with the dissipation of the excess pore water pressure increases.

It is usual in practice that for taking account of the secondary compression, the strain after the primary consolidation (ε_s) is estimated by the following equation:

$$\varepsilon_s = \frac{C_\alpha}{1+e} \log (t/t_p) \qquad (2)$$

where t_p is time of the EOP. The C_α is the coefficient of the secondary compression and may be defined by the slope of change in void ratio to time in the logarithm scale. Besides the validity of the Eq. (2), the practical problem is whether the value of C_α can be uniquely obtained by the consolidation test or not. As indicated in the companion paper (Tanaka, 2005), the C_α varies with the stress level and also with the elapsed time. In addition, as shown in Fig. 9, even at the same stress level, the C_α is influenced by the thickness of the objective layer. As shown in Fig. 9, in the case of $H=2$ cm, the value of C_α gradually increases with the increase in t/t_p until $t/t_p=30$, then C_α starts decreasing. However, when H is more than 5 cm, the C_α is decreasing with time and the absolute value of C_α is decreasing with increase in the H. This result is consistent with the fact that as H increases, the settlement due to secondary compression becomes insignificant.

Behavior of Individual Element

Unlike a specimen in a triaxial cell, the effective stress as well as the strain is not uniform in the specimen in the oedometer, since the excess pore water pressure dissipates from the drained side. The ICO test has capability to measure such p' and ε at various distances in the specimen from the drainage boundary.

Figure 10 shows the $\varepsilon - p'$ relation for the test of H10 (for the total specimen thickness of 10 cm and 5 soil elements). In these figures, p' in each element was calculated from the average of the pore water pressures measured at the both sides of the element. The ε was calculated based on the displacement of the element measured by the gap sensor. It can be seen that the initial behavior of the Element 1 in both Figs. 10 and 11 is different from that of other elements. This may be because the dissipation of the excess pore water pressure in the Element 1 is very fast. It should be noted that either the p' or the ε in Element 1 is not distributed as calculated from the two pore water pressures and displacement

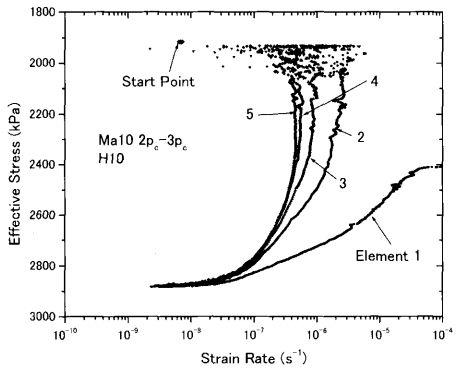

(a) Ma10: The stress range is at normally consolidated state

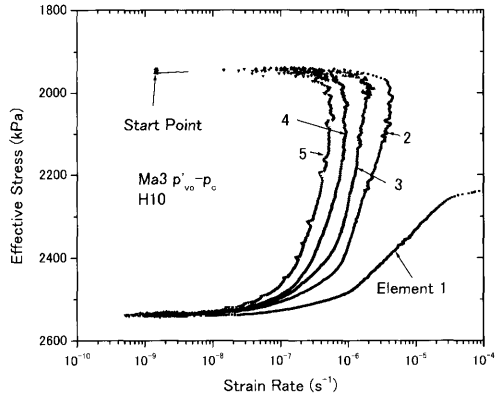

(b) Ma3: The stress range is at overconsolidated state

Fig. 11. Change in the strain rate for each element during consolidation

measured by the gap sensor. From these two figures, two important features can be recognized, i.e., non-linearity of the $\varepsilon - p'$ relation and the different relation for each element.

According to Terzaghi's consolidation theory, the strain is caused by an increase in the effective stress, and its relation is assumed to be linear. It is well known that at the normally consolidated state, the e or ε decreases with $\log p'$ from the oedometer test. Even though p' in the horizontal axis of Fig. 10(a) is plotted in the logarithm scale, the ε does not increase linearly with the increase in the $\log p'$, but the ε generated in all elements is very small until the p' of 2200 kPa. This non-linearity trend is much more prominent in Fig. 10(b), where the stress range varies from p'_{vo} to p_c.

Furthermore, the consolidation of each element does not follow a single locus in the $\varepsilon - p'$ space, but they are moving along with different loci. That is, for the element closer to the drainage boundary, the generated strain is small and most part of the ε occurs under constant effective stresses: i.e., its locus is located at right hand side in the figure.

Figure 11 shows the relationship between p' and strain rate ($\dot{\varepsilon}$), corresponding to Fig. 10. From the starting point, the $\dot{\varepsilon}$ for each element rapidly increases without recognizable change in p', then once the $\dot{\varepsilon}$ reaches the maximum value, it gradually decreases with increase in p'. When this relation for each element is looked in more detail, it can be noted that the $\dot{\varepsilon}$ for higher numbered element becomes smaller when compared with the same p'. This tendency is easily understandable because the effective stress firstly increases in the soil element close to the drained side. Therefore, it can be inferred that the difference in the relationship between p' and ε among soil elements as shown in Figs. 10(a) and (b) is due to the difference in $\dot{\varepsilon}$ for each element caused by different distance from the drainage. In this paper, such difference in the $\varepsilon - p'$ relation for each element will be explained by the strain rate theory or isotache model (for example, Imai et al., 2003; den Haan and Kamao, 2003).

In Fig. 10, points at certain strain rates ($\dot{\varepsilon}$) are plotted on the $\varepsilon - p'$ relation for each element. For the test of Ma10 in Fig. 10(a), the soil elements were preconsolidated at two times of the p_c (= 1920 kPa) and the $\dot{\varepsilon}$ at the end of the preconsolidation stage was nearly the same in each element and its value was about $8.3 \times 10^{-9}\,s^{-1}$. Since the strain in these figures is defined based on the specimen height prior to starting the objective stress range ($2p_c$ to $3p_c$), the $\dot{\varepsilon}$ at $\varepsilon = 0$ is $8.3 \times 10^{-9}\,s^{-1}$ in Fig. 10(a). The points at the same $\dot{\varepsilon}$ in each soil element during the objective stress level can be plotted in Fig. 10(a). If a line is drawn through these points, this line may be the equi-strain rate line of $8.3 \times 10^{-9}\,s^{-1}$. It may be considered that the $\varepsilon - \log p$ relation obtained by the CRS test is also an equi-strain rate line at a given $\dot{\varepsilon}$. Previous researchers, who were using mainly reconstituted soil, have revealed that the equi-strain rate lines are straight in the $\varepsilon - \log p$ space and are parallel to each other at the normally consolidated state (for example, Imai et al., 2003). Indeed, the slope of the equi-strain rate line of $8.3 \times 10^{-9}\,s^{-1}$ corresponds to the compression index (C_c) of 0.68, whose value is very close to that measured by the CRS test ($C_c = 0.65$) at this stress level. The lines with the same slope of $8.3 \times 10^{-9}\,s^{-1}$ are also drawn for other $\dot{\varepsilon}$, as shown in the figure. Although most points for the same $\dot{\varepsilon}$ are distributed in a small restricted spot of the $\varepsilon - \log p$ space, it seems that the locus for $3.3 \times 10^{-7}\,s^{-1}$ can be traced by the line with the same slope as that at $\dot{\varepsilon}$ of $8.3 \times 10^{-9}\,s^{-1}$. Therefore, equi-strain rate lines for various $\dot{\varepsilon}$ may be parallel to that of $\dot{\varepsilon} = 8.3 \times 10^{-9}\,s^{-1}$, as shown in Fig. 10(a).

Based on these lines, stress shift due to the change in $\dot{\varepsilon}$ (the rate effect on the $\varepsilon - \log p$ relation) will be examined. The number in the parenthesis for each $\dot{\varepsilon}$ indicates how to reduce the stress with a decrease in $\dot{\varepsilon}$, based on $\dot{\varepsilon}$ of the $3.3 \times 10^{-6}\,s^{-1}$. Figure 12 shows how the values of p_c are shifted by the change in $\dot{\varepsilon}$, measured by the CRS test. Here, the rate effect is defined by the ratio to the p_c at $3.3 \times 10^{-6}\,s^{-1}$ (*see* also Fig. 21 in the companion paper, Tanaka, 2005). In this figure, CRS1 is the test where the CRS test is performed at various $\dot{\varepsilon}$ for individual specimens. CRS2 used the same specimen but the strain rate was changed during testing. In this figure, the point obtained by the ICO in Fig 10(a) is plotted. These points agree surprisingly well with those measured by the CRS

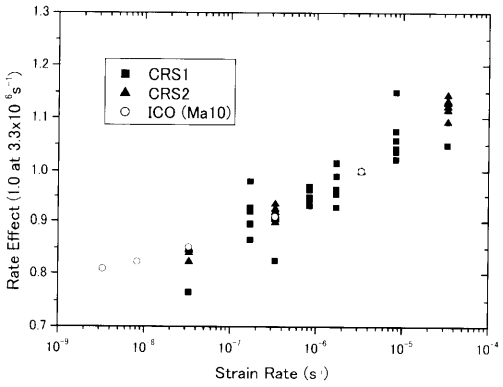

Fig. 12. The strain rate effect measured by CRS and ICO tests

tests.

The above procedure cannot be directly applied to the test result from Ma3 where the stress range is from p'_{vo} to p_c, because the equi-strain rate lines do not consist of the straight lines in this stress range. Based on the $\varepsilon - p'$ relation measured by the CRS test (the equi-strain rate line of $3.3 \times 10^{-6}\,s^{-1}$) and using the rate effect measured from Ma10 at the normally consolidated stage (in Fig. 12), a family of equi-strain rate lines is estimated by the normalization rule of Leroueil et al. (1985). They have shown that the $\varepsilon - \log p$ relation at various $\dot{\varepsilon}$ can be normalized in the form of p/p_c, where the p_c value varies with the $\dot{\varepsilon}$ according to Fig. 10(a). It is confirmed by the companion paper (Tanaka, 2005) that this normalization rule can be applied to the Osaka Pleistocene clays (*see* Fig. 19 of the companion paper). It can be seen in Fig. 10(b) that points at various $\dot{\varepsilon}$ measured by the ICO coincide fairly well with loci of equi-strain rate lines estimated by the CRS test. Therefore, it may be concluded that the isotache model is quite useful method to predict settlement including the secondary compression stage.

CONCLUSIONS

Using the Inter-Connected Oedometer (ICO) apparatus, consolidation behavior with different specimen thickness is studied under normally consolidated state and at state of transition from the in situ stress (p'_{vo}) to the yield consolidation pressure (p_c). The thickness of the specimen varies from 2 cm to 20 cm for the transition consolidation stress, i.e., from p'_{vo} to p_c, and from 2 cm to 10 cm for the normally consolidated state. Taking advantage of the ICO, relationships between the effective stress and strain with different drainage distance are also studied. The tested soils are retrieved from the Osaka Pleistocene clay layers, whose OCR may not have been created by stress history, but by the ageing or cementation.

When the stress range is at the overconsolidated state, most part of the settlement occurs after dissipation of the excess pore water pressure. However, it turned out that when the specimen is thicker, the proportion of the settlement during the dissipation of the excess pore water pressure becomes larger. The validity of the strain rate theory was confirmed by the relationships between the effective stress and strain, which vary with distance from the drainage boundary. The dependency of secondary compression on the thickness of the specimen can be explained by the strain rate theory: i.e., due to the smaller strain rate with thicker specimen, the settlement generated under the constant effective stress apparently is small. In another word, the conventional oedometer test of 2 cm thickness with double drainage sides considerably overestimates the settlement after the primary consolidation in the field, where the thickness of compressible layer is many times larger than that of the oedometer at laboratory.

REFERENCES

1) Aboshi, H. (1973): An experimental investigation on the similitude in the consolidation of a soft clay including creep settlement, *Proc. 8th ICSMFE*, **4.3**, 88.
2) Aboshi, H., Matsuda, H. and Okuda, M. (1981): Preconsolidation by separate-type consolidometer, *Proc. 10th ICSMFE*, **3**, 572–579.
3) Berre, T. and Iversen, K. (1972): Oedometer tests with different specimen heights on a clay exhibiting large secondary compression, *Geotechnique*, **22** (1), 53–70.
4) Den Haan, E. J. and Kamao, S. (2003): Obtaining isotache parameters from a C.R.S. *K*o-Oedoemeter, *Soils and Foundations*, **43** (4), 203–214.
5) Imai, G. and Tan, Y. (1992): A constitutive equation of one-dimensional consolidation derived from inter-connected tests, *Soils and Foundations*, **32** (2), 83–96.
6) Imai, G., Tanaka, Y. and Saegusa, H. (2003): One-dimensional consolidation modeling based on the isotach law for normally consolidated clays, *Soils and Foundations*, **43** (4), 173–188.
7) Itoh, Y., Takemura, K., Ishiyama, T., Tanaka, Y. and Iwaki, H. (2000): Basin formation at a contractional bend of a large trascurrent fault: Plio-Pleistocene subsidence of the Kobe and northern Osaka Basins, Japan, *Tectonophysics*, **321**, 327–341.
8) Ladd, C. C., Foott, R., Ishihara, K., Schlosser, F. and Poulous, H. G. (1977): Stress-deformation and strength characteristics, *Proc. 9th ICSMFE*, **1**, 421–494.
9) Leroueil, S., Kabbaj, M., Tavenas, F. and Bouchard, R. (1985): Stress-strain-strain rate relation for the compressibility of sensitive natural clays, *Geotechnique*, **35**, 159–180.
10) Mesri, G., Kwan Lo, D. O. and Feng, T. W. (1994): Settlement of embankments on soft clays, *Proc. Settlement '94, ASCE, GT*, 8–56.
11) Tanaka, H. (2005): Consolidation behavior of natural soils around p_c value – Long term consolidation test –, *Soils and Foundations*, **45** (3), 83–95.
12) Tanaka, H. and Locat, J. (1999): A microstructural investigation of Osaka Bay clay: the impact of microfossils on its mechanical behaviour, *Can. Getech. J.*, **36**, 493–508.
13) Tanaka, H., Ritoh, F. and Omukai, N. (2002): Quality of samples retrieved from great depth and its influence on consolidation properties, *Can. Geotech. J.*, **39**, 1288–1301.
14) Tanaka, H., Kang, M. S. and Watabe, Y. (2004): Ageing effects on consolidation properties – Based on the site investigation of Osaka Pleistocene clays –, *Soils and Foundations*, **44** (6), 39–51.